Atmospheric Pollution Research 4 (2013) 454-461

Atmospheric Pollution Research

www.atmospolres.com

Characterization of mercury in atmospheric particulate matter in the southeast coastal cities of China

Lingling Xu [1, 2], Jinsheng Chen [1], Zhenchuan Niu [1], Liqian Yin [1], Yanting Chen [1]

[1] *Key Lab of Urban Environment and Health, Institute of Urban Environment, Chinese Academy of Sciences, Xiamen 361021, China*
[2] *Graduate School of Chinese Academy of Sciences, Beijing 100049, China*

ABSTRACT

Although present in a low concentration in the atmosphere, mercury in particulate matter (PHg) plays an important role in the biogeochemical process of mercury. In this study, the mercury concentrations in three size fractions of airborne particulate matters collected from 14 sites (12 urban sites, 1 rural site and 1 remote site) in the southeast coastal cities of China during different seasons in 2010–2011 were investigated. Most of PHg (46.8–71.9%) was concentrated in the finer particles, i.e. $PM_{2.5}$ (particulate matter ≤2.5 μm in aerodynamic diameter). The average mercury concentrations in $PM_{2.5}$ were 141.2±128.1 (range of 7.6–956.5), 37.0±19.2 (5.6–89.4), and 24.0±14.6 (3.2–59.9) pg m^{-3} at urban, rural, and remote sites during the whole sampling period, respectively. The PHg concentrations were almost at the same level in spring, autumn, and winter, approximately two times of that in summer. PHg concentrations in the atmosphere displayed a significant spatial variation with far higher values in urban areas than those at rural and remote sites. The dry deposition fluxes of total PHg estimated by a theoretical model were 38.3, 47.7, and 58.7 μg m^{-2} y^{-1} at Ji'an (JA), Jimei (JM), and Longwen (LW), respectively. The backward air trajectory analysis revealed that the atmospheric PHg concentrations were mainly influenced by air masses from ocean sources that diluted PHg in summer and on contrary from continental sources in other seasons.

Keywords: *Particulate mercury, seasonal variation, spatial distribution, dry deposition flux, backward air trajectory*

Corresponding Author:
Jinsheng Chen
☎ : *+86-592-6190765*
🖷 : *+86-592-6190765*
✉ : *jschen@iue.ac.cn*

Article History:
Received: 11 June 2013
Revised: 05 September 2013
Accepted: 06 September 2013

doi: 10.5094/APR.2013.052

1. Introduction

Mercury, especially the methylated mercury, is a global pollutant that has attracted considerable attentions because of its harmful effects on human health (Schroeder and Munthe, 1998). Atmospheric mercury exists primarily as the inorganic forms that can be divided into vapor phase mercury (Hg), including Hg^0 and Hg^{2+}, and particulate Hg (PHg). Vapor phase Hg constitutes the majority of the total atmospheric mercury. Particulate Hg consists of mercury bounded or adsorbed to particulate matter in the atmosphere, which accounts for less than 10% (Xiu et al., 2005).

Hg^0 is a fairly stable form of Hg and has a long atmospheric residence time of 0.5 to 2 years (Lindqvist et al., 1991). Contrarily, once emitted from sources, Hg^{2+} is easily transferred to PHg during the transport of air masses, and is removed from the atmosphere via wet and dry deposition due to its high water–solubility and high deposition velocity (Schroeder and Munthe, 1998; Fu et al., 2008). The deposition velocity of PHg strongly depends on its particle size (Lynam and Keeler, 2005; Poissant et al., 2005). Atmospheric dry deposition is an important pathway for transferring PHg from atmosphere to the terrestrial and aquatic ecosystems (Fang et al., 2001). Although many uncertainties existed in estimating the dry deposition of PHg, the large dry deposition amounts of mercury (half or equal to wet deposition amounts) were found for many regions (Pai et al., 1997; Landis and Keeler, 2002). Moreover, previous studies have found elevated levels of mercury in pristine water bodies where there were few anthropogenic emission sources nearby (Swain et al., 1992; Rasmussen, 1994; Sorensen et al., 1994; Landis and Keeler, 2002), indicating that the atmospheric transport followed by deposition is a major pathway for the mercury contamination in remote areas (Miller et al., 2005). Therefore, although PHg is present at low levels of pg m^{-3} in the atmosphere, its behavior is crucial in mercury removal and biogeochemical processes (Lindberg and Stratton, 1998; Kim et al., 2009).

China is the largest emitter of mercury worldwide. The anthropogenic emission of mercury to air was estimated to be more than 800 tons in 2005 (Pacyna et al., 2010). Fossil fuel combustion, metal production, artisanal gold production, and cement production were responsible for the large amount of anthropogenic sources of mercury in China. In the past few decades, researches on the atmospheric PHg have been conducted in many cities such as Changchun and Beijing (Fang et al., 2001; Wang et al., 2006a) in the north of China, and Guiyang in the southwest of China (Fu et al., 2011), where were heavily polluted by coal combustion and by Hg mining and smelting, respectively. This study focused on the atmospheric PHg in southeastern China. The investigated region was selected in the southeast coastal cities of China, with the Pearl River Delta (PRD) region to the south and the Yangtze River Delta (YRD) region to the north. The objectives of this study were (1) to present the particulate Hg concentrations in the atmosphere in the Southeast coastal cities of China, (2) to characterize the spatial differences and seasonal variation of PHg concentrations, (3) to estimate the dry deposition flux by using a theoretical model, and (4) to identify the sources of air masses influencing the PHg concentrations in different seasons.

2. Materials and Methods

2.1. Site description

The sampling sites were located in the southeast coastal region of China, with most of the sites in Fujian Province. This region has a typical subtropical monsoon climate with hot summer and warm winter. The annual average temperature was 19.9 °C and the average precipitation was 1 429 mm. Northerly winds prevail in winter, while southerly winds reign in summer. The 14 sampling sites selected in eight coastal cities are showed in Figure 1. Among the 14 sampling sites, PT was located near a freshwater reservoir and it was thought to be a rural site due to the limited human activity. JXM was located at the summit of Jiuxian Mountain with an altitude of approximately 1 700 m, which was surrounded by forest. It could be considered as a remote background site. Apart from these two sites, other sites were located in the urban areas. LuC, JC, FQ, LiC, XY, FZ, LW, and SM were located in commercial and residential mixed areas. JA and LH were located in the typical residential areas. SS and JM were located in newly developed areas with many commercial or residential buildings under construction. The detailed site descriptions are given in Table 1.

2.2. Sample collection

Ten days intensive sampling campaigns were conducted simultaneously at the 14 sites in November 20–29, 2010, January 5–14, April 13–22, and August 1–10, 2011, representing autumn, winter, spring and summer, respectively. The 23–h (from 8:00 am to 7:00 am the following day) size–fractionated particulate matters ($PM_{2.5}$, $PM_{2.5–10}$, and $PM_{10–100}$: particulate matter with aerodynamic diameters <2.5, 2.5–10, and 10–100 μm, respectively) were collected simultaneously at a flow–rate of 100 L min^{-1} using a medium–volume sampler (Tianhong TH–150C Ш, China) loaded with quartz fiber filters (QFFs). In this study, a total of 558 sets of samples were collected. All of the $PM_{2.5}$, $PM_{2.5–10}$, and $PM_{10–100}$ samples at JA, JM and LW were analyzed, while at other sites, only $PM_{2.5}$ samples were analyzed. Prior to sampling, the filter was heated at 450 °C for 5 h to remove absorbed mercury. All filters were conditioned under constant temperature (25±1 °C) and relative humidity (52±1%) before and after sampling. The loaded filter was packed and sealed in polyethylene plastic bags, and stored in a refrigerator at about –20 °C.

2.3. Analytical methods and QA/QC

The mass loading was determined gravimetrically by the difference between the weights of QFFs before and after sampling with an analytical balance (Sartorius 0.01 mg, Germany). Four anions (F^-, Cl^-, SO_4^{2-}, and NO_3^-) were detected by ion chromatography (ICS–3000, Dionex, USA), and the details are given by Xu et al. (2012).

The sampled quartz filter was thermally desorbed with a PYRO–915+ pyrolysis unit and analyzed with a RA–915+ analytical equipment based on Zeeman atomic absorption spectrometry (Lumex, Russia). Compared with the traditional glass fiber filtration–acid digestion–cold–vapor atomic absorption spectrometry (CVAAS) or cold–vapor atomic fluorescence spectrometry (CVAFS) method, thermal desorption has an advantage of no addition of any chemicals or reagents. Thermal desorption were also widely used in AES Minitrap device developed by Lu et al. (1998) and Tekran 1135 unit manufactured by Tekran Instruments Corporation. It should be noted that manual sample transfer and sampling handing might lead to a slight loss or gain of PHg during the pyrolysis process. Therefore, much careful sampling process and a clean room facility were required to avoid contamination.

Table 1. *Description of 14 sampling sites in the southeast coastal cities of China*

Location (City, Province)	Site [a]	Longitude, Latitude	Sampling height (m)	N	Category	Description
Wenzhou, Zhejiang	LuC	28.01, 120.27	20	40	Urban	Represents a residential and commercial environment of urban area
Ningde, Fujian	JC	26.66, 119.54	21	40	Urban	Represents a residential and commercial environment of urban area
Fuzhou, Fujian	JA	26.08, 119.32	30	40	Urban	Located at urban center area, about 30 m away from the main traffic road
	FQ	25.73, 119.39	20	40	Urban	On the roof of the monitoring station of Fuqing city
	PT	25.49, 119.76	10	40	Rural	A managed station of reservoir, the pollution was least
Putian, Fujian	LiC	25.46, 119.00	20	37	Urban	On the roof of the monitoring station of Putian city
	XY	25.32, 119.10	30	40	Urban	On the roof of a building in the government of Xiuyu district; represents a residential and commercial environment of urban area
Quanzhou, Fujian	FZ	24.90, 118.60	30	42	Urban	On the roof of monitoring station of Quanzhou Environmental Protection Bureau; represents a residential environment
	SS	24.73, 118.66	25	40	Urban	On the roof of a building in a high school
	JXM	25.71, 118.11	2	40	Remote	Located at the summit of Jiuxian Mountain with an altitude of about 1 700 m
Xiamen, Fujian	JM	24.61, 118.06	5	40	Urban	Located at the institute of urban environment, CAS; about 30 m away from the main traffic roads; a lot of municipal construction work is going, near the Xinglin Bay
	SM	24.48, 118.15	20	40	Urban	On the roof of a building in a primary school; about 100 m away from the main traffic road
Zhangzhou, Fujian	LW	24.51, 117.72	15	38	Urban	Represents an industrial, commercial and traffic mixed environment
Shantou, Guangdong	LH	23.36, 116.72	18	41	Urban	Represents a cultural and educational area

[a] *Site full names: LuC, LuCheng; JC, Jiaocheng; JA, Jin'an; FQ, Fuqing; PT, Pingtan; LiC, Licheng; XY, Xiuyu; FZ, Fengze; SS, Shishi; JXM, Jiuxian mountain; JM, Jimei; SM, Siming; LW, Longwen; LH, Longhu.*

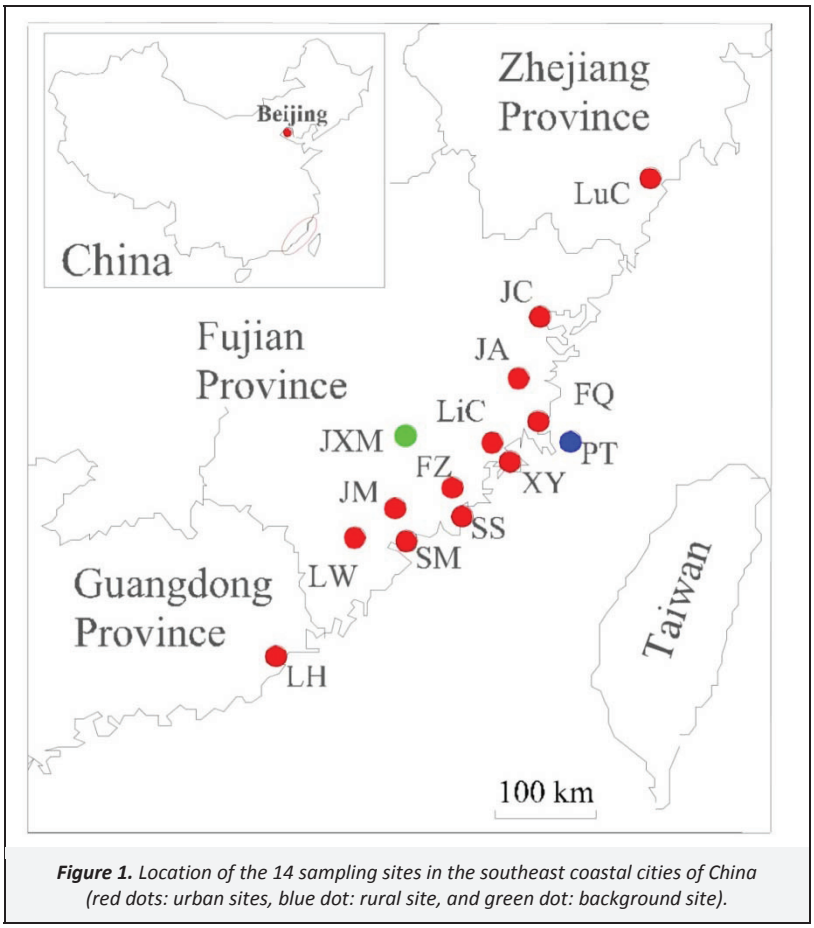

Figure 1. *Location of the 14 sampling sites in the southeast coastal cities of China (red dots: urban sites, blue dot: rural site, and green dot: background site).*

The average PHg concentration in the blank filter was 1.9±1.2 ng g^{-1} and the blank amount was subtracted from the sample amount. The blank filter was prepared the same manner as the sampling filters except that no air was taken. The PHg mass content per unit particles mass (C_m, ng g^{-1}) was converted to PHg mass per unit air volume (C_v, pg m^{-3}) by Equation (1):

$$C_v = \frac{C_m \times m}{V} \quad (1)$$

where *m* is the particle mass of analyzed sample; *V* is the sampling volume (0 °C, 1.01×10^5Pa).

The standard reference materials were purchased from Lumex, Russia for the quality assurance purposes. Recoveries of standard material were between 90.7 and 109.0%, and the average relative standard deviation on precision test was 3.1%. A quality control sample was prepared and analyzed for every 20 samples. Each sample was determined twice, and the precision of PHg for sample replicate was within ±10%, and the mean value was used finally.

2.4. Statistically analysis

The correlation analysis was carried out using SPSS for Windows version 17.0. The one–way ANOVA test was used to determine the differences in PHg concentrations among different locations and among different seasons.

3. Results and Discussion

3.1. PHg concentration

The concentrations of particulate mercury in $PM_{2.5}$ at urban, rural, and remote sites from 2010 to 2011 are summarized in Table 2. The average PHg concentrations (range) were 141.2±128.1 (7.6–956.5) pg m^{-3}, 37.0±19.2 (5.6–89.4) pg m^{-3} and 24.0±14.6 (3.2–59.9) pg m^{-3} at urban, rural and remote sites during the sampling period, respectively. The average concentration of PHg at urban sites was approximately 6 times of that at remote site, suggesting that the more significance of anthropogenic Hg sources in urban areas. The level of atmospheric PHg concentration in the southeast coastal cities of China was much higher than the northern hemisphere background value (<1.0–5.0 pg m^{-3}) (Jaffe et al., 2005).

The PHg concentrations in the southeast coastal cities were compared to the data from other Chinese cities and foreign cities. It should be pointed out that different analytical methods could largely affect the accuracy of analytical values, which has been explained by Wang et al. (2006a). The results showed that PHg concentrations at urban sites in the southeast coastal cities were considerably lower than those in other cities of China, such as Guiyang, Beijing, and Shanghai. This might correspond to the less emission from human activity in the study region (Wu et al., 2006). The PHg concentrations in urban areas were 5.9–11.3 folds higher than the values reported from the adjacent Asian country (Seoul, Korea), North America (Detroit, USA) and Europe (Goteborg, Sweden), indicating that a large amount of anthropogenic mercury was released to the atmosphere in China.

3.2. Size distribution of Hg in PM at urban sites

The average concentrations and percentages of mercury in three size–fractioned particles, i.e. $PM_{2.5}$, $PM_{2.5–10}$, and $PM_{10–100}$ at three urban sites (JA, JM, and LW) during the different seasons are shown in Figure 2. It could be found that the PHg concentrations decreased significantly with the increase of particle size in all of the seasons. The highest percentages of PHg were found in $PM_{2.5}$, accounting for 67.7% of the total particulate mercury in spring,

46.8% in summer, 71.9% in autumn, and 67.3% in winter, respectively. Among the three urban sites, JM and LW had the similar seasonal variation with higher PHg concentration in $PM_{2.5}$ in autumn, while JA had relatively low amount in autumn compared to other seasons (Figure 3). The differences of Hg in $PM_{2.5}$ for different locations would be further discussed in the following section. The percentages of mercury in $PM_{2.5}$ were a little lower than those observed in Detroit and Chicago, USA (Pirrone et al., 1996), where mercury in $PM_{2.5}$ contributed 85% and 70% to the total particulate mercury, respectively. It was obviously found that the difference between mercury in fine particles ($PM_{2.5}$) and in coarse particle (PM with size >2.5) was much significant in spring, autumn, and winter than that in summer. This could be explained by that PHg from coal combustion mainly existed in fine particles and this fraction was markedly reduced in summer (Pirrone et al., 1995a). Apart from directly emitted, atmospheric PHg might have two formation mechanisms: Adsorption of gaseous mercury in particles and chemical gas–particle transformation (Xiu et al., 2005). Mercury in coarse particles might be generally associated with adsorption of gaseous mercury in coarse particles, while mercury in fine particles were formed through the two processes as above. High temperature and strong solar radiation in summer might be in favor of the gas–particle transformation. But on the other hand, it accelerated the release of mercury from different environmental surfaces, such as water and soil surfaces, which was easily adsorbed on coarse particles (Zhang et al., 2010). Therefore, the size distribution of mercury in different seasons might be a result of both primary mercury emissions and secondary mercury formation.

3.3. Spatial distribution of Hg in $PM_{2.5}$

The concentrations of PHg in $PM_{2.5}$ at the 14 sites during four seasons are shown in Figure 3. A statistically significant spatial variation of PHg in $PM_{2.5}$ was observed among sampling locations (ANOVA test; $p<0.05$). The high levels of PHg were found at LW, JM, LuC, and JC, while the lower PHg concentrations were present at JXM and PT. Limited human activity at rural site (PT) and remote site (JXM) might result in the extremely low PHg concentrations. Elevated PHg concentration at urban sites might associate to the anthropogenic emission. LuC and JC were located in the central area of cities, where the rapid industrialization was under–way (Xu et al., 2013). Strong emission from coal combustion for industrial and commercial use might account for the highest PHg concentration at LW. As a newly developed area, JM had large amount commercial and residential buildings under construction, which led to a more serious pollution state.

The seasonal variation pattern was quite different among these locations (Figure 3). Two of the urban sites, JM and LW, had a similar seasonal distribution of Hg in $PM_{2.5}$. PHg concentrations peaked at LW during winter and summer, which were 12.0 and 5.4 times higher than that at JXM, respectively. In spring and autumn, the highest PHg concentrations were observed at LuC and JM, about 12.8 and 25.0 times of the values at JXM in each season. The seasonal pattern for LuC had much in common with JC, JA, FQ, XY, and FZ, which had the highest PHg concentration in $PM_{2.5}$ in spring and the lowest PHg in summer. These sites were found to be mainly distributed in the north of the study region. We noticed that the elevation of JM and LW were lower than other urban sites, which probably influenced the Hg variability especially during the ground–based measurement. The similar seasonal pattern was observed for LiC and SS. The seasonal PHg concentrations in $PM_{2.5}$ at SM and LH were both in the following order: winter > autumn > spring > summer.

3.4. Seasonal variability of Hg in $PM_{2.5}$

The seasonal concentrations of PHg in $PM_{2.5}$ at individual sampling sites are shown in Figure 3. There was a statistically significant difference in PHg concentration among different seasons (ANOVA test; $p<0.05$). The PHg concentrations were lowest in summer at all the sampling sites, which might be due to the less coal combustion and wood burning for heating in the hot season. Atmospheric PHg concentration in summer might be influenced by the air masses coming from the ocean. The most mercury was emitted in the species of Hg^0 from ocean and contributed less to PHg. Conversely, the clean air masses could dilute the PHg concentration to a great extent. In addition, the wet precipitation was higher in frequency and intensity in summer, scavenging a large amount of PHg in the ambient air.

Table 2. *Comparison of atmospheric PHg concentrations among different cities*

Location	Classification	Time	Particulate Fraction	PHg concentration (pg m^{-3})			Reference
				Range	Mean	S.D.	
Southeast coastal cities of China [a]	Urban	Nov. 2010, Jan., Apr., and Aug. 2011	$PM_{2.5}$	7.6–956.5	141.2	128.1	This study
	Rural		$PM_{2.5}$	5.6–89.4	37.0	19.2	
	Remote		$PM_{2.5}$	3.2–59.9	24.0	14.6	
Guiyang [b]	Urban	Aug. to Dec. 2009	$PM_{2.5}$	0–8 407	368	676	(Fu et al., 2011)
Beijing [c]	Urban	Jan.–Dec. 2003	TSP	180–3 510	1 180	820	(Wang et al., 2006a)
Shanghai [d]	Urban	Apr. to May 2005	TSP	200–470	330.0	90.0	(Xiu et al., 2009)
Mt. Changbai [b]	Remote	Aug. 2005 to Jul. 2006	$PM_{2.5}$	0–1 001	77	136	(Wan et al., 2009)
Seoul, Korea [e]	Urban	Feb. 2005 to Feb. 2006	$PM_{2.5}$		23.9	19.6	(Kim et al., 2009)
Göteborg, Sweden [f]	Urban	2005	$PM_{2.5}$	3.9–20.3	12.5	5.9	(Li et al., 2008)
Québec, Canada [b]	Rural	1 Jan. to 12 Dec. 2003	$PM_{2.5}$		26	54	(Poissant et al., 2005)
Detroit, USA [b]	Urban	2003	$PM_{2.5}$		20.8	30.0	(Liu et al., 2007)

[a] *Lumex RA–915+/PYRO–915+*
[b] *Tekran 2537/1130/1135*
[c] *Manual sampling and acid digestion, CVAFS*
[d] *Manual sampling and acid digestion, CVAAS*
[e] *Manual sampling and thermal desorption, CVAFS*
[f] *Manual sampling and thermal desorption (AES Mini trap), AFS*

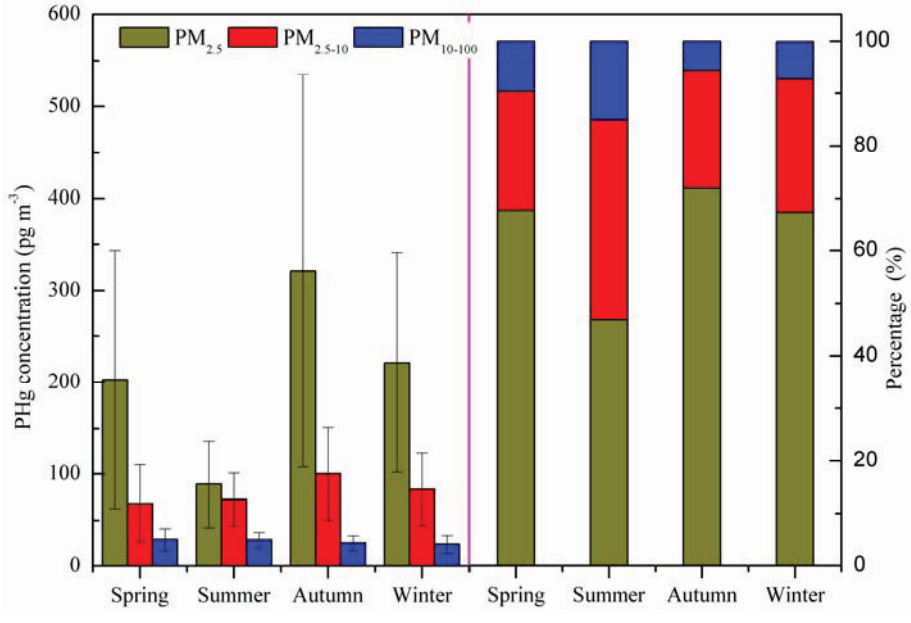

Figure 2. *Distribution of the average concentrations and percentages of mercury in size–fractionated particles at three urban sites (JA, JM, and LW).*

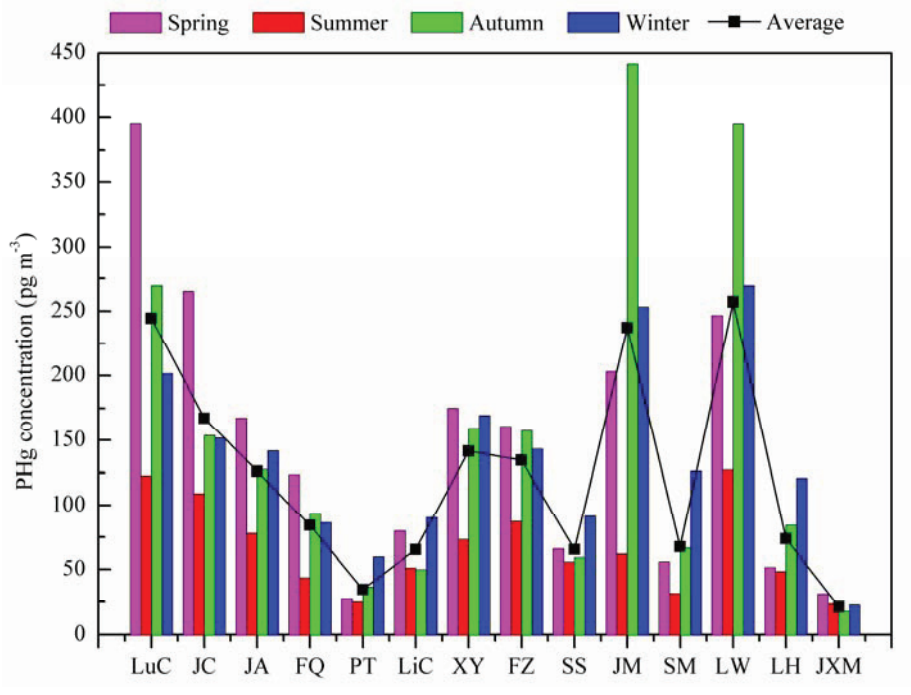

Figure 3. *Spatial and seasonal variation of PHg concentration in $PM_{2.5}$ during the sampling period.*

It was found that the PHg concentrations in winter were not evidently higher than those in spring and autumn at the most of sampling sites. This seasonal variation did not agree well with the previous results that exhibited the extremely elevated PHg concentrations in winter (Fang et al., 2001; Wang et al., 2006a; Liu et al., 2007; Fu et al., 2008). Several reasons might explain this. First, during the sampling month in winter, i.e. January, the region had an average temperature around 7–10 °C. Therefore, less coal or wood combustion for heating might have released less mercury to the atmosphere in this region. The sampling period in autumn and spring in this study occurred during the times of heating season beginning (in mid November) and ended (in mid March) in the northern cities of China, hence, the northwest monsoon might carry a great amount of particulate matters with condensed mercury to the southeast coastal cities in spring and autumn, besides in winter, which would be confirmed by backward trajectory analysis.

The correlations between PHg and other pollutants (F^-, Cl^-, SO_4^{2-}, and NO_3^-) are depicted in Table 3. Inorganic mercury might exist in particles through various mercury compounds such as Hg^0, Hg_2Cl_2, $HgCl_2$, $HgSO_4$, HgS, and HgO. Hg^+ was unstable and readily oxidized to Hg^{2+}. Hg^0 contributed to the volatile PHg, $HgSO_4$ and HgS contributed to the stable inert PHg, and $HgCl_2$ and HgO contributed to the reactive PHg (Xiu et al., 2005). A strong correlation was observed between PHg and Cl^- during sampling period, especially in spring, autumn, and winter. This suggested that Hg^{2+} was the significant form of mercury existed in particles.

The PHg were found to be strongly correlated to SO_4^{2-} in spring and autumn. As we know, SO_4^{2-} was a typical tracer of coal combustion. The close correlation between PHg and SO_4^{2-} indicated the significant contribution of coal combustion. The relative lower correlation coefficient between PHg and SO_4^{2-} was found in winter than other seasons, suggesting other important contributions besides coal combustion in winter. The close correlations between PHg and NO_3^- were observed in spring, autumn, and winter. NO_3^- was an indicator of traffic source. The previous study found that gasoline vehicles contributed a substantial amount of mercury to the atmosphere (Landis et al., 2007).

Table 3. *Correlations between PHg and other pollutants (F^-, Cl^-, SO_4^{2-}, and NO_3^-) in different seasons*

		F^-	Cl^-	SO_4^{2-}	NO_3^-
Spring	R(Hg–X)	0.09	0.70[b]	0.31[b]	0.44[b]
	N[a]	138	138	138	138
Summer	R(Hg–X)	0.20[c]	0.22[b]	0.24[b]	0.21[c]
	N	139	139	139	138
Autumn	R(Hg–X)	–0.02	0.53[b]	0.45[b]	0.36[b]
	N	140	140	140	140
Winter	R(Hg–X)	0.30[b]	0.69[b]	0.27[b]	0.33[b]
	N	140	140	140	140

[a] *Number of the samples*
[b] *Correlation is significant at the 0.01 level (2–tailed)*
[c] *Correlation is significant at the 0.05 level (2–tailed)*

3.5. Dry deposition fluxes

The dry deposition fluxes of contaminants to a receptor surface have been estimated by models. Modeled estimates are typically generated by multiplying the concentrations of contaminants by the dry deposition velocity of particles. The dry deposition flux of PHg to a receptor surface was evaluated by using the Equation (2) (Holsen and Noll, 1992):

$$F = \sum C_i V_i \quad (2)$$

where F is the dry deposition flux, C_i is the PHg concentration in the atmosphere, and V_i is the dry deposition velocity. The dry deposition velocity was influenced by meteorological conditions (i.e., wind speed, humidity, ambient temperature, and atmospheric stability), receptor surface characteristics (i.e., surface roughness) and particle characteristics (i.e., aerodynamic particle diameter, particle density, and shape). The dry deposition velocity of coarse particles was generally higher than that of fine particles, higher in summer than that in winter and higher in industrial and commercial areas than in residential areas (Pirrone et al., 1995b).

In this study, the dry deposition fluxes of mercury at JA, JM, and LW during different seasons were estimated based on several assumptions (Table 4). The ten daily PHg concentrations were averaged to a seasonal value due to the limited sampling time in this study. Therefore, it should be noted that the estimate of annual dry deposition flux may have a large uncertainty. At the same time, the dry deposition velocity was assumed to be dependent on particle size distribution and the site differences rather than seasonal variation and meteorological conditions. JA was an urban center site with transportation as the major emission source, JM was a coastal urban site, and LW was an industrial site. According to the Zhang et al. (2012) for different types of sites, the dry deposition velocity of $PM_{2.5}$, $PM_{2.5–10}$, and $PM_{10–100}$ were 0.14, 0.20, and 3.96 cm s^{-1} at JA, 0.12, 0.20, and 3.75 cm s^{-1} at JM, and 0.19, 0.21, and 4.31 cm s^{-1} at LW during the study period, respectively. As showed in Table 4, the average annual dry deposition fluxes of total PHg were 38.3, 47.7, and 58.7 μg m^{-2} y^{-1} at JA, JM and LW respectively. The seasonal variation of deposition fluxes was similar to the pattern in the seasonal variation of the PHg concentrations. The dry deposition fluxes of total PHg in urban areas in the southeast coastal cities of China were about 2–4 times of that in Central Europe and Northern Europe (17.5 μg m^{-2} y^{-1}) (Petersen et al., 1995).

Table 4. *Summary of dry deposition fluxes of PHg at JA, JM, and LW during different seasons*

Site	Flux (μg m^{-2} $season^{-1}$)				Annual (μg m^{-2} y^{-1})
	Spring	Summer	Autumn	Winter	
JA	10.8	9.3	8.1	10.0	38.3
JM	10.7	10.1	14.9	12.0	47.7
LW	16.3	14.1	16.4	11.8	58.7

3.6. Backward trajectory analysis

It is well known that air masses travelling from different regions bring different chemical components with the aerosols, thus components among different air masses can shed some light on their possible sources (Wang et al., 2006b; Kong et al., 2010). In this study, a–week air parcel backward trajectories at JM (N: 24.61, E: 116.72) were computed at 100, 500, and 1 000 m AGL for different seasons (NOAA, 2013). In the HYSPLIT model, the air masses at 100, 500, and 1 000 described the air flow and atmospheric characteristic of the ground surface layer, the boundary layer, and the upper boundary layer, respectively. JM was selected as the representative site because it was affected by air masses from the ocean, and has been undergoing the rapid economic development.

The results of backward air trajectory analysis are presented in Figure 4. Very different origins of the air masses arrived at JM at different levels and at different seasons were observed. In spring, the air masses at 500 and 1 000 m heights originated from Russia while the trajectory at a lower height of 100 m came from Kazakhstan. They all passed through the Mongolia and the northeastern inland of China. The heating season generally began in late November and lasted to mid March in northern China, thus the air masses brought a large amount of mercury emitted from coal combustion and finally elevated the PHg concentrations in the investigated areas during spring. The western air parcels were observed in autumn and winter. The trajectories at higher altitudes (1 000 m) were identified that air masses originated from or passed through the India, but the trajectories arriving at the lower altitudes were a little different between these two seasons. In autumn, the air parcel at 500 m was from the Kazakhstan with passing through the most of inland of western China. The air parcel at 100 m was from the area around the study region. While in winter, the air condition at JM was influenced by the relatively clean air masses from the Southeast Asian Countries. It was reported that some provinces in western China where the air parcels passed through, such as Guizhou and Sichuan province, contributed considerable amount of mercury to the atmosphere (Wu et al., 2006). India ranked the second greatest anthropogenic contributor of mercury worldwide following China (Pacyna et al., 2010). Therefore, it was reasonable that the PHg concentrations in winter were comparable to those in spring and autumn mentioned in the previous sections. Totally different trajectories were found during summer. In this season, the trajectories originated from the Indian Ocean with passing the South China Sea and finally arrived at the study site. Contrasting to the air masses from continent, the ocean air masses led to the decrease in PHg concentrations to some extent.

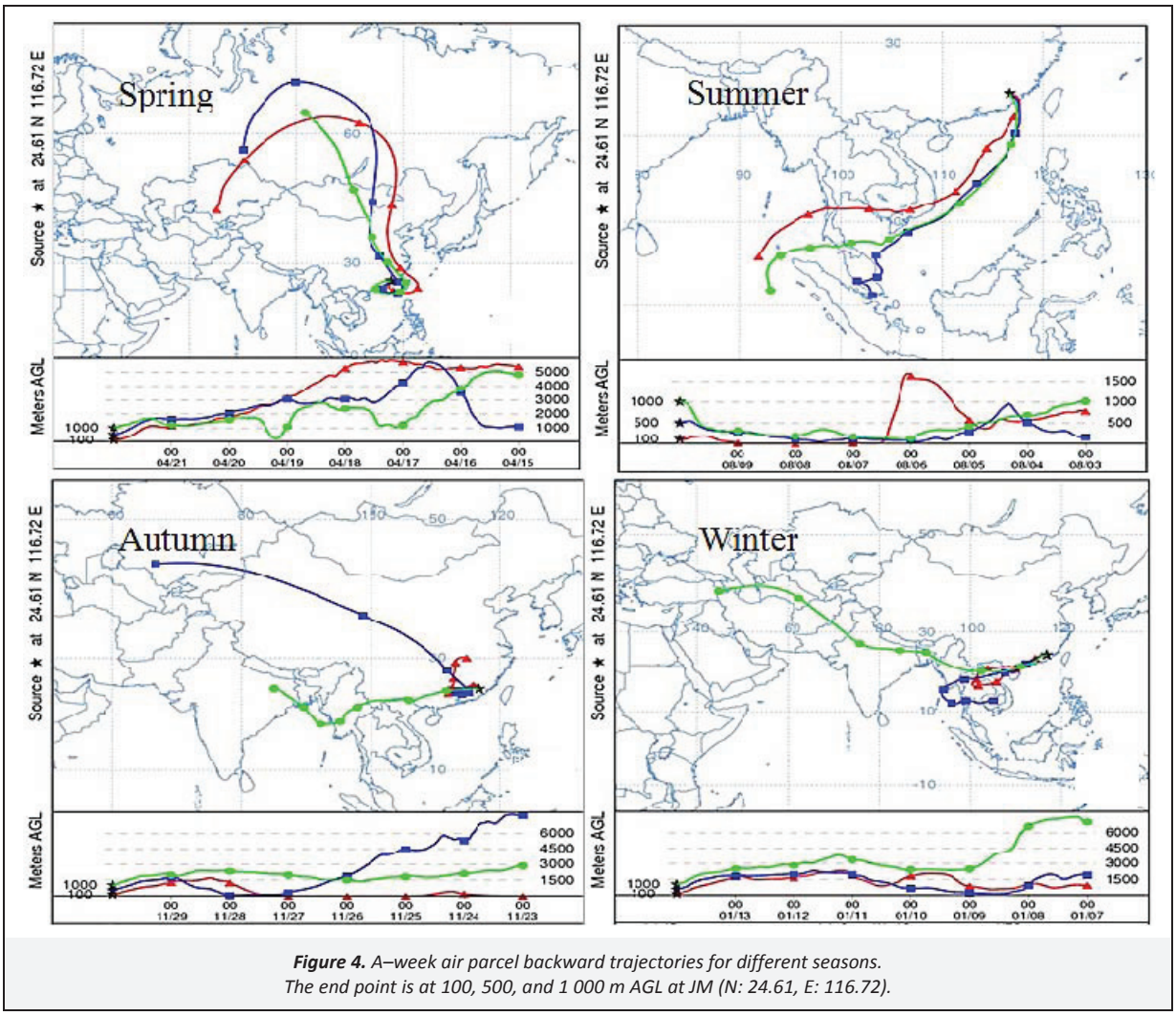

Figure 4. *A–week air parcel backward trajectories for different seasons. The end point is at 100, 500, and 1 000 m AGL at JM (N: 24.61, E: 116.72).*

4. Conclusions

The results of size distribution revealed that most of the PHg existed in fine particles, accounting for 46.8–71.9% of the total particulate mercury. The average concentrations of mercury in $PM_{2.5}$ were 141.2±128.1, 37.0±19.2, and 24.0±14.6 pg m^{-3} at urban, rural, and remote sites during the sampling period, respectively, which were much higher than the background value. In urban areas, the annual dry deposition fluxes of total PHg estimated by a theoretical model were 38.3, 47.7, and 58.7 μg m^{-2} y^{-1} at JA, JM, and LW, respectively.

The higher concentrations of Hg in $PM_{2.5}$ were observed at urban sites than those at rural and background sites. The lower PHg concentration was present in summer comparing to other seasons. A similar seasonal pattern was observed at JM and LW, which had extremely high PHg concentration in autumn. The seasonal variability of PHg at LuC had much in common JC, JA, FQ, XY, and FZ. These locations were mainly distributed in the North of study region.

The backward air trajectory analysis indicated that air masses arriving at the study site mainly originated from ocean sources, and thus diluted the PHg concentration in the atmosphere in summer. The PHg concentrations were influenced mainly by air masses from continental Russia or India or China in other seasons. This might be the main reason for the results that the comparable PHg concentrations were observed in spring, autumn, and winter, but remarkably higher than that in summer.

Acknowledgments

This research was financially supported by the Natural Science Foundation of Fujian Province, China (no. 2013J05063), the National Natural Science Foundation of China (no. 41303072), and the Knowledge Innovation Program of Chinese Academy of Sciences (No: KZCX2–EW–408).

References

Fang, F.M., Wang, Q.C., Li, J.F., 2001. Atmospheric particulate mercury concentration and its dry deposition flux in Changchun City, China. *Science of the Total Environment* 281, 229–236.

Fu, X.W., Feng, X.B., Qiu, G.L., Shang, L.H., Zhang, H., 2011. Speciated atmospheric mercury and its potential source in Guiyang, China. *Atmospheric Environment* 45, 4205–4212.

Fu, X.W., Feng, X.B., Zhu, W.Z., Zheng, W., Wang, S.F., Lu, J.Y., 2008. Total particulate and reactive gaseous mercury in ambient air on the eastern slope of the Mt. Gongga area, China. *Applied Geochemistry* 23, 408–418.

Holsen, T.M., Noll, K.E., 1992. Dry deposition of atmospheric particles – application of current models to ambient data. *Environmental Science & Technology* 26, 1807–1815.

Jaffe, D., Prestbo, E., Swartzendruber, P., Weiss–Penzias, P., Kato, S., Takami, A., Hatakeyama, S., Kajii, Y., 2005. Export of atmospheric mercury from Asia. *Atmospheric Environment* 39, 3029–3038.

Kim, S.H., Han, Y.J., Holsen, T.M., Yi, S.M., 2009. Characteristics of atmospheric speciated mercury concentrations (TGM, Hg(II) and Hg(p)) in Seoul, Korea. *Atmospheric Environment* 43, 3267–3274.

Kong, S.F., Han, B., Bai, Z.P., Chen, L., Shi, J.W., Xu, Z., 2010. Receptor modeling of $PM_{2.5}$, PM_{10} and TSP in different seasons and long–range transport analysis at a coastal site of Tianjin, China. *Science of the Total Environment* 408, 4681–4694.

Landis, M.S., Keeler, G.J., 2002. Atmospheric mercury deposition to Lake Michigan during the Lake Michigan Mass Balance Study. *Environmental Science & Technology* 36, 4518–4524.

Landis, M.S., Lewis, C.W., Stevens, R.K., Keeler, G.J., Dvonch, J.T., Tremblay, R.T., 2007. Ft. McHenry tunnel study: source profiles and mercury emissions from diesel and gasoline powered vehicles. *Atmospheric Environment* 41, 8711–8724.

Li, J., Sommar, J., Wangberg, I., Lindqvist, O., Wei, S.–Q., 2008. Short–time variation of mercury speciation in the urban of Göteborg during GÖTE–2005. *Atmospheric Environment* 42, 8382–8388.

Lindberg, S.E., Stratton, W.J., 1998. Atmospheric mercury speciation: concentrations and behavior of reactive gaseous mercury in ambient air. *Environmental Science & Technology* 32, 49–57.

Lindqvist, O., Johansson, K., Aastrup, M., Andersson, A., Bringmark, L., Hovsenius, G., Hakanson, L., Iverfeldt, A., Meili, M., Timm, B., 1991. Mercury in the Swedish environment – recent research on causes, consequences and corrective methods. *Water Air and Soil Pollution* 55, xi–261.

Liu, B., Keeler, G.J., Dvonch, J.T., Barres, J.A., Lynam, M.M., Marsik, F.J., Morgan, J.T., 2007. Temporal variability of mercury speciation in urban air. *Atmospheric Environment* 41, 1911–1923.

Lu, J.Y., Schroeder, W.H., Berg, T., Munthe, J., Schneeberger, D., Schaedlich, F., 1998. A device for sampling and determination of total particulate mercury in ambient air. *Analytical Chemistry* 70, 2403–2408.

Lynam, M.M., Keeler, G.J., 2005. Automated speciated mercury measurements in Michigan. *Environmental Science & Technology* 39, 9253–9262.

Miller, E.K., Vanarsdale, A., Keeler, G.J., Chalmers, A., Poissant, L., Kamman, N.C., Brulotte, R., 2005. Estimation and mapping of wet and dry mercury deposition across northeastern North America. *Ecotoxicology* 14, 53–70.

NOAA (National Oceanic and Atmospheric Administration), 2013. http://ready.arl.noaa.gov/HYSPLIT.php, accessed in June 2013.

Pacyna, E.G., Pacyna, J.M., Sundseth, K., Munthe, J., Kindbom, K., Wilson, S., Steenhuisen, F., Maxson, P., 2010. Global emission of mercury to the atmosphere from anthropogenic sources in 2005 and projections to 2020. *Atmospheric Environment* 44, 2487–2499.

Pai, P., Karamchandani, P., Seigneur, C., 1997. Simulation of the regional atmospheric transport and fate of mercury using a comprehensive Eulerian model. *Atmospheric Environment* 31, 2717–2732.

Petersen, G., Iverfeldt, A., Munthe, J., 1995. Atmospheric mercury species over central and northern Europe – model–calculations and comparison with observations from the Nordic air and precipitation network for 1987 and 1988. *Atmospheric Environment* 29, 47–67.

Pirrone, N., Keeler, G.J., Allegrini, I., 1996. Particle size distributions of atmospheric mercury in urban and rural areas. *Journal of Aerosol Science* 27, 13–14.

Pirrone, N., Glinsorn, G., Keeler, G.J., 1995a. Ambient levels and dry deposition fluxes of mercury to Lakes Huron, Erie and St Clair. *Water Air and Soil Pollution* 80, 179–188.

Pirrone, N., Keeler, G.J., Warner, P.O., 1995b. Trends of ambient concentrations and deposition fluxes of particulate trace metals in Detroit from 1982 to 1992. *Science of the Total Environment* 162, 43–61.

Poissant, L., Pilote, M., Beauvais, C., Constant, P., Zhang, H.H., 2005. A year of continuous measurements of three atmospheric mercury species (GEM, RGM and Hg–p) in southern Quebec, Canada. *Atmospheric Environment* 39, 1275–1287.

Rasmussen, P.E., 1994. Current methods of estimating atmospheric mercury fluxes in remote areas. *Environmental Science & Technology* 28, 2233–2241.

Schroeder, W.H., Munthe, J., 1998. Atmospheric mercury – an overview. *Atmospheric Environment* 32, 809–822.

Sorensen, J.A., Glass, G.E., Schmidt, K.W., 1994. Regional patterns of wet mercury deposition. *Environmental Science & Technology* 28, 2025–2032.

Swain, E.B., Engstrom, D.R., Brigham, M.E., Henning, T.A., Brezonik, P.L., 1992. Increasing rates of atmospheric mercury deposition in midcontinental North America. *Science* 257, 784–787.

Wan, Q., Feng, X.B., Lu, J., Zheng, W., Song, X.J., Li, P., Han, S.J., Xu, H., 2009. Atmospheric mercury in Changbai Mountain area, northeastern China II. The distribution of reactive gaseous mercury and particulate mercury and mercury deposition fluxes. *Environmental Research* 109, 721–727.

Wang, Z.W., Zhang, X.S., Chen, Z.S., Zhang, Y., 2006a. Mercury concentrations in size–fractionated airborne particles at urban and suburban sites in Beijing, China. *Atmospheric Environment* 40, 2194–2201.

Wang, Y., Zhuang, G.S., Zhang, X.Y., Huang, K., Xu, C., Tang, A.H., Chen, J.M., An, Z.S., 2006b. The ion chemistry, seasonal cycle, and sources of $PM_{2.5}$ and TSP aerosol in Shanghai. *Atmospheric Environment* 40, 2935–2952.

Wu, Y., Wang, S.X., Streets, D.G., Hao, J.M., Chan, M., Jiang, J.K., 2006. Trends in anthropogenic mercury emissions in China from 1995 to 2003. *Environmental Science & Technology* 40, 5312–5318.

Xiu, G.L., Cai, J., Zhang, W.Y., Zhang, D.N., Bueler, A., Lee, S.C., Shen, Y., Xu, L.H., Huang, X.J., Zhang, P., 2009. Speciated mercury in size–fractionated particles in Shanghai ambient air. *Atmospheric Environment* 43, 3145–3154.

Xiu, G.L.L., Jin, Q.X., Zhang, D.N., Shi, S.Y., Huang, X.J., Zhang, W.Y., Bao, L., Gao, P.T., Chen, B., 2005. Characterization of size–fractionated particulate mercury in Shanghai ambient air. *Atmospheric Environment* 39, 419–427.

Xu, L.L., Yu, Y.K., Yu, J.S., Chen, J.S., Niu, Z.C., Yin, L.Q., Zhang, F.W., Liao, X., Chen, Y.T., 2013. Spatial distribution and sources identification of elements in $PM_{2.5}$ among the coastal city group in the Western Taiwan Strait region, China. *Science of the Total Environment* 442, 77–85.

Xu, L.L., Chen, X.Q., Chen, J.S., Zhang, F.W., He, C., Zhao, J.P., Yin, L.Q., 2012. Seasonal variations and chemical compositions of $PM_{2.5}$ aerosol in the urban area of Fuzhou, China. *Atmospheric Research* 104, 264–272.

Zhang, L., Fang, G.C., Liu, C.K., Huang, Y.L., Huang, J.H., Huang, C.S., 2012. Dry deposition fluxes and deposition velocities of seven trace metal species at five sites in central Taiwan – a summary of surrogate surface measurements and a comparison with model estimations. *Atmospheric Chemistry and Physics* 12, 3405–3417.

Zhang, F.W., Zhao, J.P., Chen, J.S., Xu, Y., 2010. Distribution characteristics of particulate mercury in aerosol in coastal city. *Huan Jing Ke Xue* 31, 2273–2278 (in Chinese).